ASIAN JOURNAL OF CIVIL ENGINEERING (BUILDING AND HOUSING) VOL. 11, NO. 4 (2010)
PAGES 477-494

MEAN AND FLUCTUATING WIND LOADS ON AN INDUSTRIAL STRUCTURE WITH CURVED ROOF

A. Abraham, S. Arunachalam*, S. Selvi Rajan, G. Ramesh Babu and N. Lakshmanan
CSIR-Structural Engineering Research Centre, Chennai-113, India

ABSTRACT

A wind tunnel pressure measurements study was carried out to obtain the pressure distribution on a model (1:200) of an industrial structure with multi-segmental curved roof, under simulated open terrain conditions. The roof of the model was instrumented with pressure taps (area averaged) beneath and above the roof surfaces for both cases i.e., model with and without gable end walls. Pressure data were collected simultaneously beneath and above the roof surfaces of the model for various angles of wind incidence ($\theta = 0°$ to $360°$ in steps of every $30°$). In this paper, results pertaining to mean ($\overline{C}_{pi}$, $\overline{C}_{pe}$) and standard deviation ($\widetilde{C}_{pi}$, $\widetilde{C}_{pe}$) of internal and external pressure coefficients for flow direction from parallel ($\theta = 0°$) to perpendicular ($\theta = 270°$) to the axis of the arch, for both cases are presented. The effect of gable end walls on $\overline{C}_{pe}$ and $\widetilde{C}_{pe}$ was also studied. Further, comparison of measured C_{pe} for flow direction $\theta = 0°$ and $270°$ to the axis of the roof with the values given in various national/international codes of practice were also presented.

Keywords: Pressure measurements; curved roof; gable end walls; angles of wind incidence; external pressure coefficients

1. INTRODUCTION

Arch shaped roofs are increasingly used in-built environment where large unobstructed clear spans (Ex: entertainment centres, exhibition centres, sports arenas, hangers, etc) are required for functionality purposes. Such structures can spring either from ground or at an elevated level. Wind loads are important load criteria in design of such structures. Currently available information of wind loads on curved roofs is limited either from wind tunnel measurements or CFD based numerical techniques. Most of the information given in literature pertains to external pressure coefficients on curved roof structures for wind direction perpendicular to the ridge. The rise (f) to span (d) ratio '(f/d)' is strongly affecting the aerodynamic loads on curved roofs. The side wall height (h) to span ratio '(h/d)' and building length (*l*) to span

* E-mail address of the corresponding author: sarun@sercm.org (S. Arunachalam)

ratio '(*l*/d)' are two other geometric parameters, which have lesser effects on wind induced loads when compared to (f/d). Since the pattern of the actual load distribution on such roofs are so complex and moreover each structure will be a 'case by case' problem, wind tunnel tests are required and recognised as a reliable design tool for evaluating aerodynamic behavior and wind induced pressures over the curved roof structures. In this paper, an attempt was made to understand the distribution of pressures and the effect of gable end walls in a model with multi-segmental curved roof, when it is subjected to a 3D flow field.

2. LITERATURE REVIEW ON CURVED ROOF

Various national/international codes of practice/published data of [1-7] specify the external pressure coefficients for curved roof structures for flow in both directions (i.e., wind blowing parallel and perpendicular to the axis of the arch) and some international codes of practice of [8, 9] specify the external pressure coefficients only for wind blowing perpendicular to the axis of the arch. Values of wind pressure coefficients for different shapes of curved roofs were reported by Krishna [10]. Based on a wind tunnel study, results on mean pressure coefficients (corresponds to wind speed applying at the eaves height) were reported by Kasperski [11], for flow direction perpendicular to axis of the building models, with (f/d) of 0.1 and 0.2, (h/d) of 0.2 and (l/d) of 1.5. The pressure coefficients through a series of parametric wind tunnel model studies were reported by Blackmore and Tsokri [12], for flow near perpendicular to axis, for (f/d) of 0.05 to 0.5, (h/d) of 0.06 to 1.0 and (l/d) of 1 to 10. The evaluated pressure coefficients were compared with international codes of practice of [3, 9], and published data of [6], and was proposed an alternative procedure to replace the EN1991-1-4 [9] recommended procedure in the UK National Annex. The influence of roof curvature on the conical vortex pattern appearing on a curved roof, when subject to oblique winds was experimentally analysed for with and without parapets at the windward curved edge of the roof by testing the mean pressure distribution on the curved roofs of low-rise building models in a wind tunnel, was reported by Franchini et al. [13], for (f/d) of 0 to 0.17, (h/d) of 0.25 and (l/d) of 1.0. Wind tunnel tests were carried out by Holmes [14] on a roof of a hanger to determine the peak values of different load effects and comparisons were made of the results with the wind loads derived from AS/NZS: 1170.2: 2002 [2]. The influence exerted by canopies on the pressure distribution over arch-roof industrial buildings was investigated by Paluch et al. [15] through BLWT, for (f/d) of 0.1, 0.2 and 0.3, (h/d) of 0.125 and 0.25, (l/d) of 2.0. Wind tunnel model studies were carried out to determine the wind load distribution on tributary areas near the gable-end of large, low-rise buildings with high pitch planar and curved roof shapes by Ginger [16], for (f/d) of 0.33, (h/d) of 0.5, (l/d) of 4.0. Wind tunnel tests were carried out to determine the wind load distribution on curved roofs for both isolated and coupled models with equal or different heights and were reported by Blessmann [17]. The experimental tests carried out in the BLWT for the design of large roofs of the new Olympic stadium (Karaiskaki) in Pyraeus (Greece), Manfredonia (Italy) and Delle Alpi of Turin (Italy) was reported by Biagini et al. [18]. An evaluation of distribution of the air pressure (for speeds of wind were analyzed

between 30 m/s and 40 m/s) is determined throughout the curved and open self-weighted metallic roof due to the wind effect by the Finite Element Method and comparison of the results obtained with the Spanish and European Standards rules, were reported by Del Coz Díaz et al. [19]. Wind tunnel pressure measurements study was carried out to obtain mean pressure coefficients on rigid models of rectangular shape buildings with cylindrical roofs as well as wall surfaces was reported by Gupta and Amareshwar [20]. Wind tunnel experiments conducted on an arch structure and on a flat-roof structure, to facilitate reliable design of such structures, pressure data were obtained from the Jules Verne climatic wind tunnel at CSTB, Nantes, where each was clad in turn in an impermeable plastic film, an 'insect net' of 33% open area, and a 'shade net' of 39% open area and was reported by Robertson et al. [21]. The results pertaining to mean 'net' pressure coefficients on a multi-segmental curved roof model with gable end walls in open case, for three typical angles of wind incidence (i.e., $\theta = 0°$, 315° and 270°), for end arches (a1 and a8) and centre arch (a4) of the roof was reported by Lakshmanan et al. [22]. The results on C_{pe} for the above typical angles of wind incidence, for the above arches in the model with and without gable end walls and comparison of C_{pe} with national/international codes of practice was reported by Abraham et al. [23]. Further, data analysis was carried out for other arches in skewed angles of wind incidence viz. $\theta = 330°$ and 300° and keeping in view of the reader's benefit, the results on (i) $\overline{C}_{pi}$ (and $\overline{C}_{pe}$) and $\widetilde{C}_{pi}$ (and $\widetilde{C}_{pe}$), (ii) $\overline{C}_{p,net}$ for model with and without gable end walls were complied for $\theta = 0°$, 330°, 315°, 300° and 270° and presented in this paper. In addition, comparison of measured C_{pe} with values given in various national/international codes of practice for roof (i) springing from ground level and (ii) on elevated structure are also presented.

3. WIND TUNNEL EXPERIMENTAL PROGRAM

3.1 Model fabrication and instrumentation

A model scale of 1:200 of an industrial structure (coal shed) with multi-segmental curved roof was fabricated using acrylic sheets. For instrumentation purpose, the roof of the model was fabricated by joining 1 mm and 3 mm thick acrylic sheets of same width and length. The model has a span of 559 mm, length of 564 mm and eaves height of 11.80 mm. Thus, it leads to (f/d) of 0.245, (h/d) of 0.021 and (l/d) of 1.01. The schematic diagram of the model tested in wind tunnel is shown in Figure 1. Since the roof profile consists of 16 segments, joined together to form a curve like shape and hence the arch is not a smooth curve (i.e., either parabola or circular in nature).

Since the coal shed model is a typical structure where external pressures above the roof and internal pressures under the roof are required to be measured to obtain 'net' pressure coefficients, $C_{p,net}$, a special method of instrumentation was adopted in this study. Manifold with five pressure taps as input was provided on the upper side of the roof at a given segment in 1 mm thick sheet. Diametrically in plan, opposite on the inner side of the roof (i.e., in 3 mm thick sheet), another set of 5 taps manifold was provided with a slightly staggered arrangement, which is shown in Figure 2.

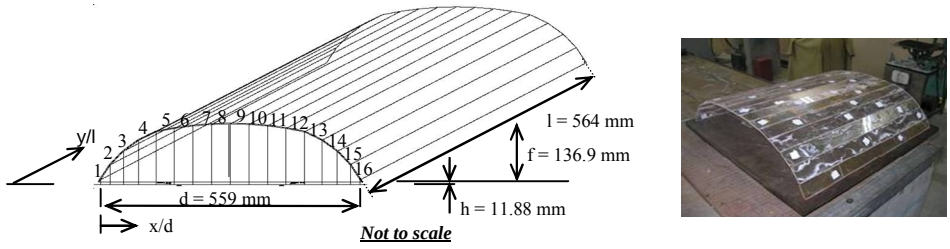

Figure 1. Schematic diagram of a multi-segmental curved roof model with dimension

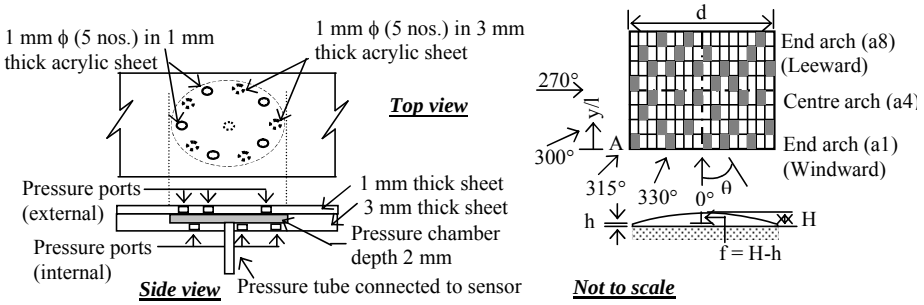

Figure 2. Manifold details under/above the roof surfaces and angles of wind incidence

From this arrangement, internal or external pressures can be measured separately by temporarily closing all the taps above the roof or by closing all the taps beneath the roof and opening all the taps above the roof.

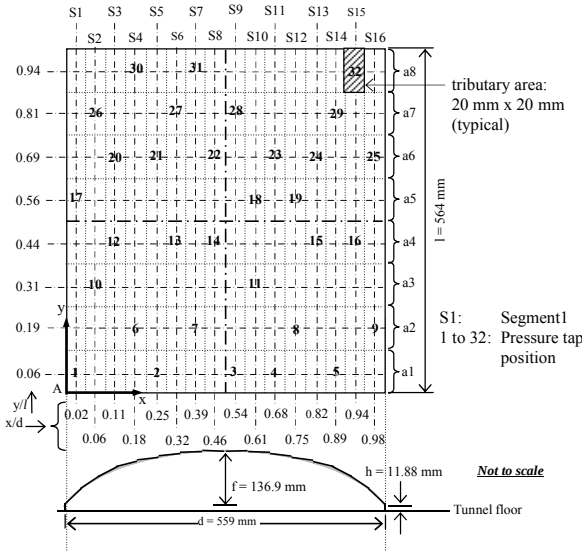

Figure 3. Relative position of pressure taps at the roof

In order to avoid cluster of tubes leading to excessive blockage effect in the model, a total no. of 32 pressure ports was used, and were judiciously distributed on the curved surface of the model (Figure 3). It may be noted that due to symmetry of the structure, when the arch is rotated from $\theta = 0^{\circ}$ to 360°, the above arrangement of pressure taps permits deduction of pressures on the entire roof of the model.

3.2 Wind tunnel tests and data processing

The tests were conducted in the state-of-the-art BLWT facility available at SERC, Chennai, under simulated open terrain conditions. The details of the test program are given below:

Sl. No	Experiment Code No. (ECN)	Case(s)	Status of pressure taps
1	ECN1	Without gable end walls	External close & Internal open
2	ECN2	Without gable end walls	External open & Internal close
3	ECN3	With gable end walls	External open & Internal close

Profiles of the mean velocity and turbulence intensity for the simulated wind are shown in Figure 4.

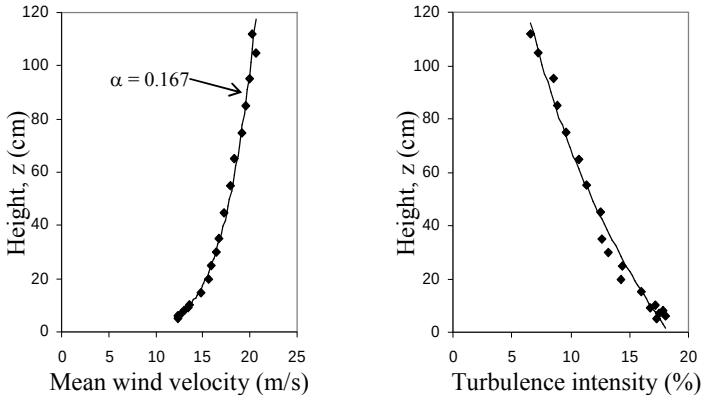

Figure 4. Characteristics of the simulated wind

For any given angle of wind incidence, simultaneous pressures were measured from 16 taps using two pressure scanners. The model was tested for different angles of wind incidence from $\theta = 0°$ to 360° in steps of every 30°. Experiments were also conducted for few other selected skew angles of wind incidence (i.e., $\theta = 45°$, 135°, 225° and 315°). Typical views of the model tested in the wind tunnel are shown in Figure 5. The simulated mean velocity of about 12 m/s measured at the crown height is taken as reference velocity V_{ref}, and all the pressure coefficients are based on reference dynamic pressure q_c,

corresponding to the above reference wind velocity. All the pressure data were acquired for a sampling period of 15 seconds with a sampling frequency of 1000 Hz. Three data runs were considered for every test case. All the pressure data were analysed using an in-house developed software.

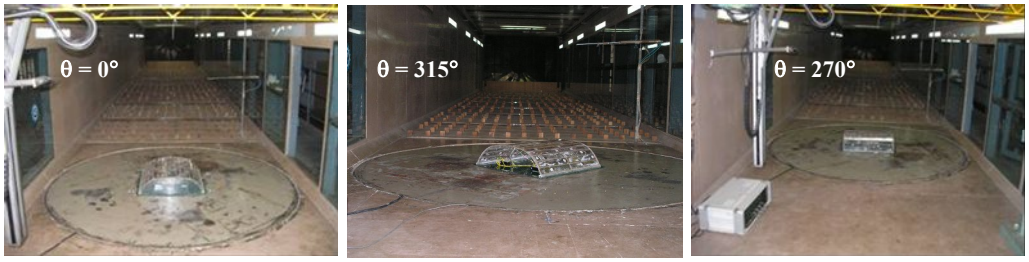

Figure 5. Typical views of the model tested in ABL wind tunnel

In this paper, results pertaining to C_{pi} and C_{pe} beneath and above the surface of the roof model with and without gable end walls, for angles of wind incidence viz. θ = 0°, 330°, 315°, 300° and 270° are presented and discussed in the following sections.

4. RESULTS AND DISCUSSIONS

4.1 ECN: 1 Distribution of mean $\overline{C}_{pi}$ and standard deviation $\widetilde{C}_{pi}$ of internal pressure coefficients: (for model with no gable end walls)

The mean $\overline{C}_{pi}$ and standard deviation $\widetilde{C}_{pi}$ of internal pressure coefficients, are obtained as given below:

$$\overline{C}_{pi} = \frac{\overline{p}_{int}}{(1/2 \rho \overline{V}_{ref}^2)} \text{ and } \widetilde{C}_{pi} = \frac{\widetilde{p}_{int}}{(1/2 \rho \overline{V}_{ref}^2)} \quad (1)$$

where, $\overline{p}_{int}$, $\widetilde{p}_{int}$ mean and standard deviation of internal pressures; $\left(1/2 \rho \overline{V}_{ref}^2\right)$ = reference pressure (q_c) due to mean wind speed at the crown of the model. The variation of $\overline{C}_{pi}$ and $\widetilde{C}_{pi}$ beneath the surface of the multi-segmental curved roof for angles of wind incidence from θ = 0º to 270º (i.e., flow direction from parallel to perpendicular to the ridge) are shown in Figure 6 and the following observations were made:

(i) For wind direction parallel (i.e., θ = 0º) to the axis of the arch, the inner surface of the entire roof is subjected to suction and the suction pressures are gradually increasing from windward arch (a1) to leeward arch (a8).

(ii) For skewed angles of wind incidence (i.e., θ = 330º, 315º, and 300º), it is interesting

to note that the distribution of $\overline{C}_{pi}$ changes from suction (at the windward region) and subsequently, to pressure at the leeward region. This phenomenon is significant at the arches (a1 and a2).

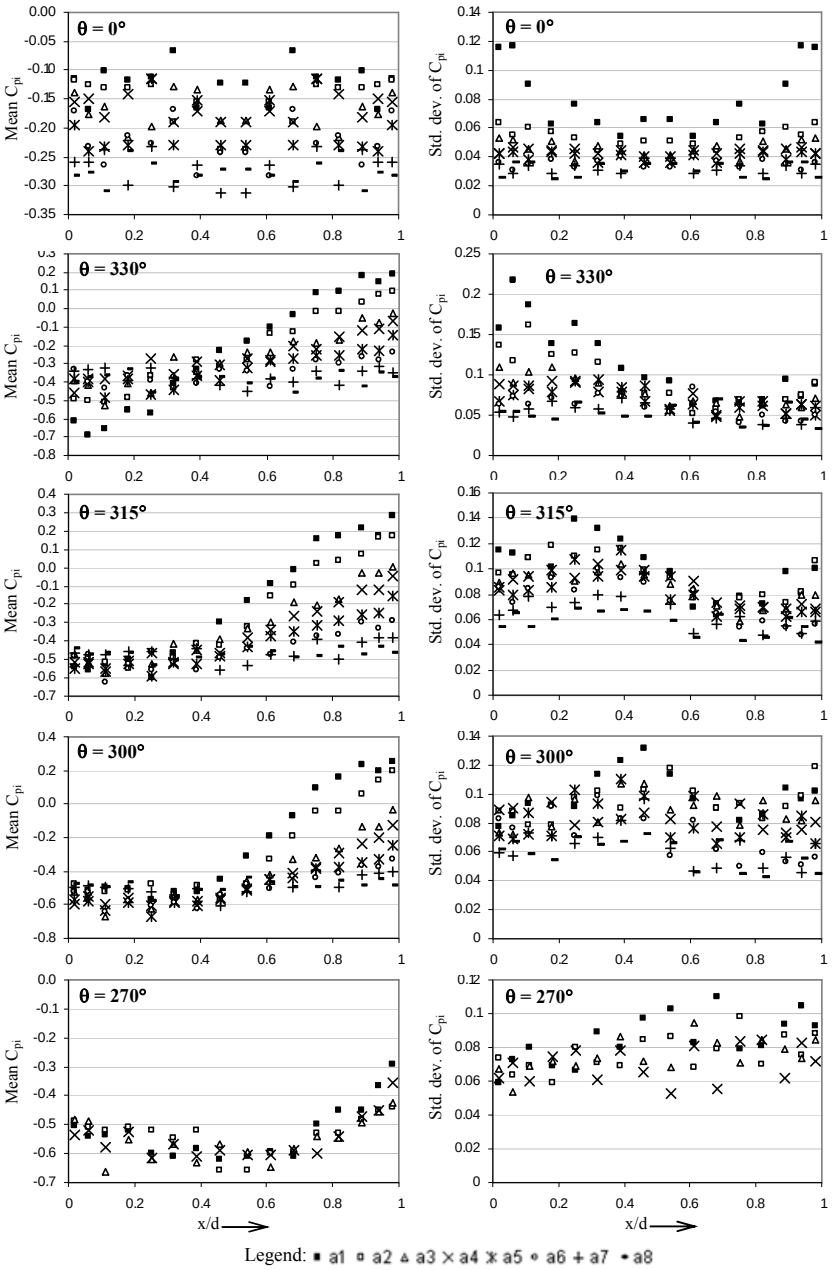

Figure 6. Variation of $\overline{C}_{pi}$ and $\widetilde{C}_{pi}$ at the inner surface of the roof (with no gable end walls)

(iii) The variation of $\overline{C}_{pi}$ at the leeward region stabilizes gradually beyond x/d = 0.5 with respect to angles of wind incidence so that the pressure recovery rate is slow when the flow direction was in the perpendicular (θ = 270º) to the axis of the arch.

(iv) For wind direction perpendicular (θ = 270º) to the axis of arch, the underneath surface of the entire roof is subjected to suction.

(v) The variation of $\widetilde{C}_{pi}$ are found to be significant at the end arch (a1) especially for θ = 0º and 330º, could be due to the edge effect and this could not be seen when the flow direction was in the perpendicular (θ = 270º) to the axis of the arch.

4.2 ECN: 2 Distribution of mean $\overline{C}_{pe}$ and standard deviation $\widetilde{C}_{pe}$ of external pressure coefficients: (for model with no gable end walls)

The mean $\overline{C}_{pe}$ and standard deviation $\widetilde{C}_{pe}$ of external pressure coefficients are obtained as given below:

$$\overline{C}_{pe} = \frac{\overline{p}_{ext}}{(\frac{1}{2}\rho \overline{V}_{ref}^{2})} \text{ and } \widetilde{C}_{pe} = \frac{\widetilde{p}_{ext}}{(\frac{1}{2}\rho \overline{V}_{ref}^{2})} \quad (2)$$

where, $\overline{p}_{ext}$, $\widetilde{p}_{ext}$ = mean and standard deviation of external pressures. The variation of $\overline{C}_{pe}$ and $\widetilde{C}_{pe}$ above the surface of the multi-segmental curved roof for angles of wind incidence from θ = 0º to 270º (i.e., flow direction from parallel to perpendicular to the ridge) are shown in Figure 7 and the following observations were made:

(i) It can be seen form Figure 7 that the magnitudes of $\overline{C}_{pe}$ were affected depending upon the flow direction.

(ii) For wind direction parallel (θ = 0º) to the axis of arch, the external surface of the entire roof is subjected to suction and the variation of $\overline{C}_{pe}$ is symmetric about the longitudinal axis of the arch. It is interesting to note that the suction pressures are gradually decreasing from windward arch (a1) to leeward arch (a8).

(iii) For other angles of wind incidence (θ = 330º, 315º, 300º and 270º), the variation of $\overline{C}_{pe}$ at leeward region of the roof is high when compared to other regions for all θ except θ = 0º and the distribution of $\overline{C}_{pe}$ show positive pressure coefficients for a small region on windward region which changes into suction pressures for rest of the roof portions.

(iv) Further, it is observed that for skewed angle of wind incidence (θ = 300º), a value of $\overline{C}_{pe}$ attains a maximum (-1.09) at the downstream of apex of the centre arch (a4), i.e., at x/d = 0.75 and y/*l* = 0.56, could be due to separation phenomenon.

(v) The variation of $\widetilde{C}_{pe}$ at the edges of windward arch (a1) is found to be significant for θ = 0º and this effect at the leeward edge in arches (a1 and a2) was sustaining even upto the flow direction was 300º.

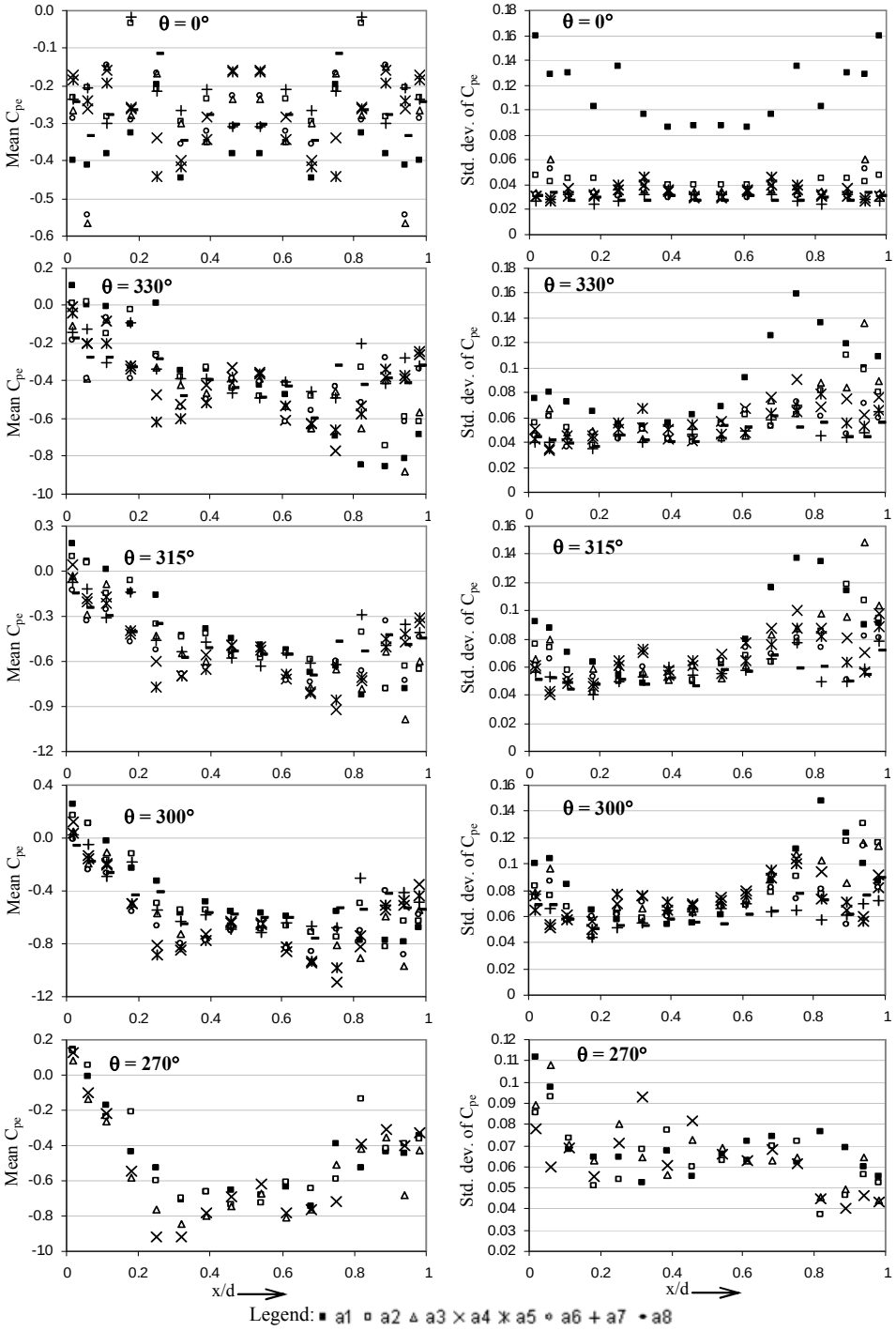

Figure 7. Variation of $\overline{C}_{pe}$ and $\widetilde{C}_{pe}$ at the outer surface of the roof (with no gable end walls)

4.3 Distribution of mean 'net' pressure coefficients, $\overline{C}_{p,net}$ (for model with no gable end walls)

The mean 'net' pressure coefficients $\overline{C}_{p,net}$ are obtained as given below:

$$\overline{C}_{p,net} = \overline{C}_{pe} - \overline{C}_{pi} \tag{3}$$

The variation of $\overline{C}_{p,net}$ for the multi-segmental curved roof with no gable end walls for angles of wind incidence from θ = 0º to 270º (i.e, flow direction from parallel to perpendicular to the ridge) are shown in Figure 8. At this juncture, the author's would like to mention that the magnitude of $\widetilde{C}_{pi}$ or $\widetilde{C}_{pe}$ found to be less when compared to $\overline{C}_{pi}$ or $\overline{C}_{pe}$, and therefore only the distribution of $\overline{C}_{p,net}$ are presented in this paper.

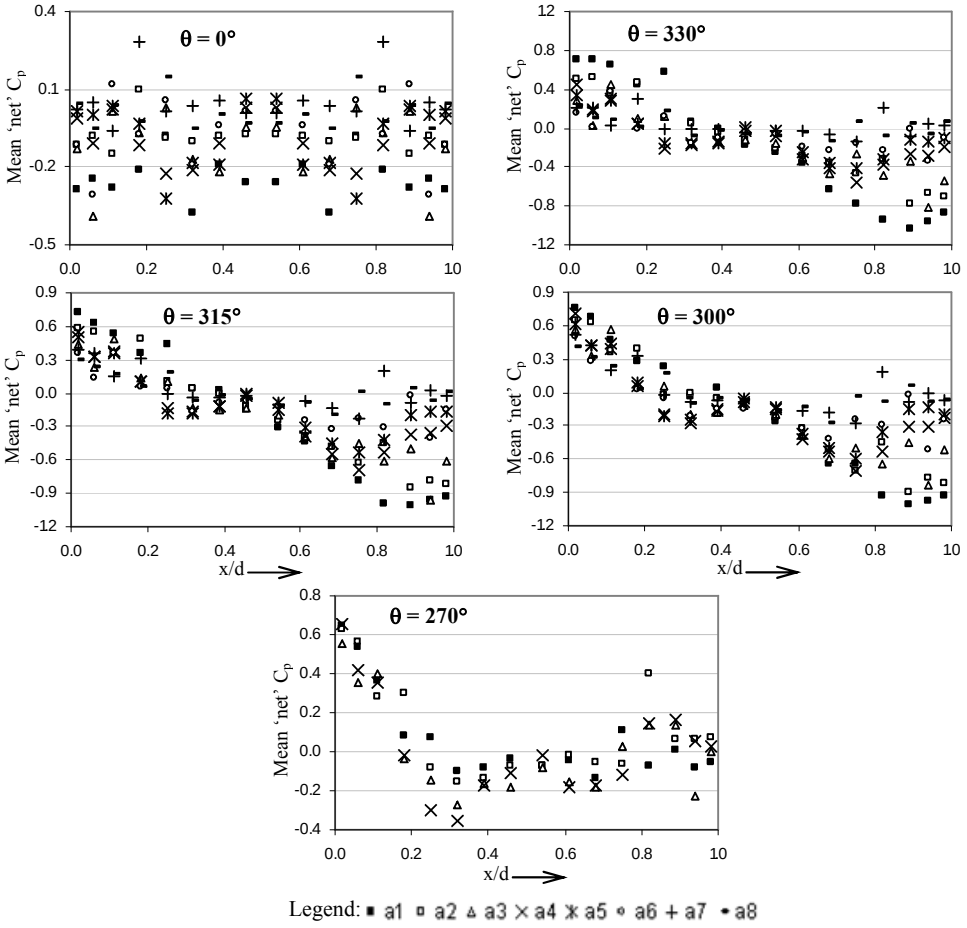

Figure 8. Variation of $\overline{C}_{p,net}$ for the entire roof of the model (with no gable end walls)

4.4 ECN: 3 Distribution of mean $\overline{C}_{pe}$ and standard deviation $\widetilde{C}_{pe}$ of external pressure coefficients: (for model with gable end walls)

The variation of $\overline{C}_{pe}$ and $\widetilde{C}_{pe}$ above the surface of the multi-segmental curved roof for angles of wind incidence from θ=0º to 270º (i.e., flow direction from parallel to perpendicular to the ridge) are shown in Figure 9 and the following observations were made:

(i) For wind direction parallel (θ=0º) to the axis of arch, the exterior surface of the entire roof is subjected to suction. It is interesting to note that the suction pressures are high at windward arch (a1) and gradually decreasing to leeward arch (a8).

(ii) For skewed wind direction (θ = 300º), a value of $\overline{C}_{pe} = -1.433$, attains maximum at the downstream of apex of the arch (a1), i.e., at x/d = 0.75 and y/*l* = 0.56.

(iii) For θ = 330º, 315º, 300º and 270º, the distribution of $\overline{C}_{pe}$ show positive pressure coefficients for a small region on windward side of the roof, which changes into suction pressures for rest of the roof portions, as in the case of ECN: 2.

(iv) For θ = 0º, the distribution of $\widetilde{C}_{pe}$ for arches a2 to a8 are similar but varying in magnitudes, whereas deviation is found for windward arch (a1). It is also interesting to note that the peak value of $\widetilde{C}_{pe}$ is shifting along the arch direction (especially at x/d = 0.32, 0.54 and 0.68 with $\widetilde{C}_{pe}$ = 0.25, 0.27 and 0.28) for θ = 330º, 315º and 300º.

5. EFFECT OF GABLE END WALLS ON $\overline{C}_{pe}$ AND $\widetilde{C}_{pe}$ OF THE ROOF SURFACE

Based on the variation of $\overline{C}_{pe}$ and $\widetilde{C}_{pe}$ for every angle of wind incidence (results not presented here) in both ECN: 2 and 3, the following observations were derived:

(i) For θ = 0º, the values of $\overline{C}_{pe}$ at windward arch (a1) for model with gable end walls are high when compared to model with no gable end walls and this effect is gradually reducing at the leeward arch (a8). For θ = 330º, 315º and 300º, the values of $\overline{C}_{pe}$ at the arch (a1) for model with gable end walls are less when compared to model with gable end walls. For θ = 270º, the variation of $\overline{C}_{pe}$ is almost similar in both cases, especially in centre arch (a4).

(ii) For θ = 0º, the values of $\overline{C}_{pe}$ at windward arch (a1) for model with gable end walls are high when compared to model with no gable end walls and this effect is gradually reducing at the leeward arch (a8).

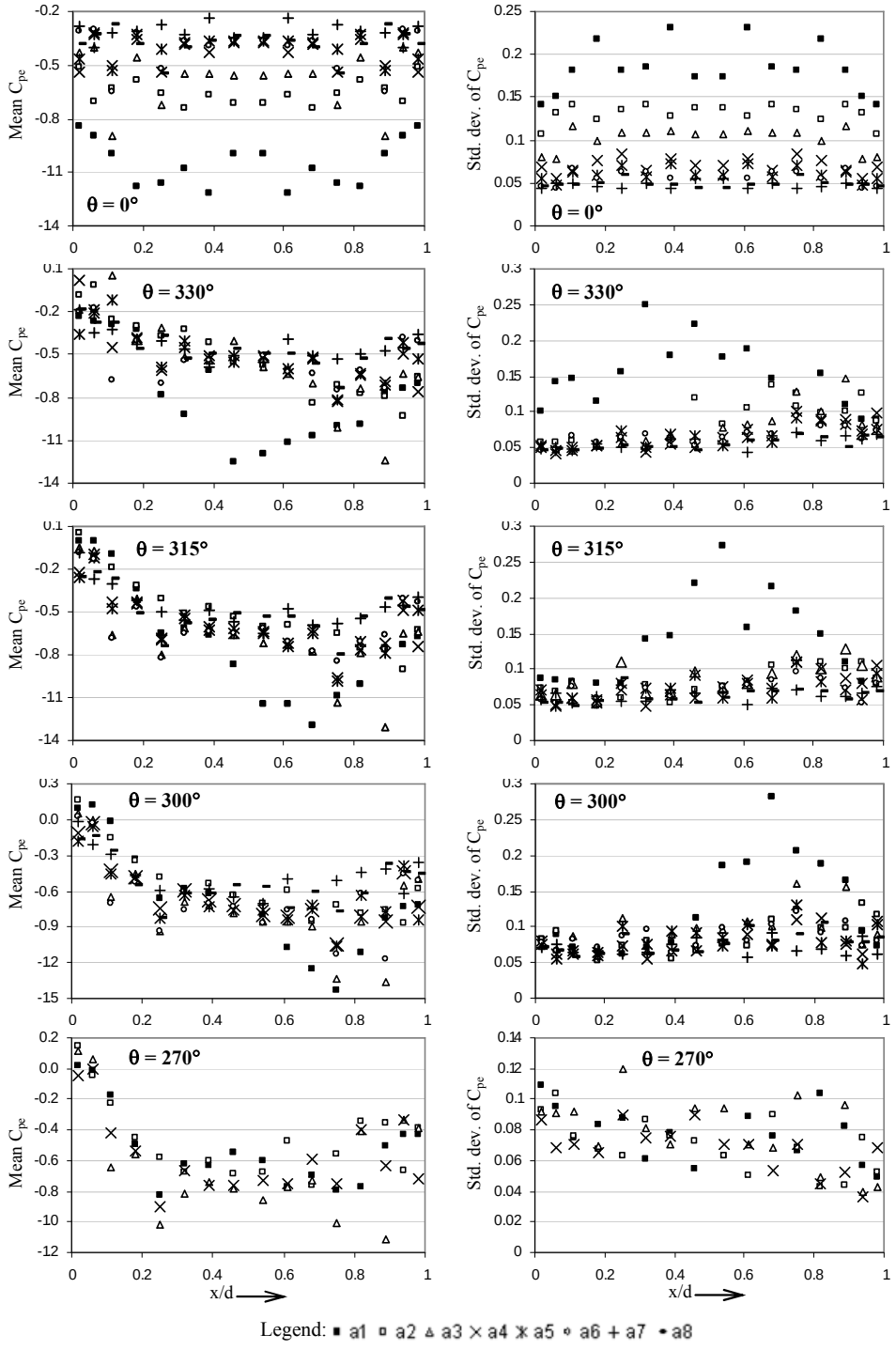

Figure 9. Variation of $\overline{C}_{pe}$ and $\widetilde{C}_{pe}$ exterior surface of the roof (with gable end walls)

(iii) For θ = 300º, a maximum value of $\overline{C}_{pe}$ = −1.09 at the downstream of apex of the centre arch (a4) in the model with no gable end walls whereas a maximum value of $\overline{C}_{pe}$ = −1.433 was found at the downstream of apex of the end arch (a1) in the model with gable end walls, at the same location (i.e., at x/d = 0.75 and y/*l* = 0.56).

(iv) For θ = 300º, a maximum value of $\overline{C}_{pe}$ = 0.249 at the arch (a1) (i.e., at x/d = 0.02 and y/*l* = 0.06) was observed in the model with no gable end walls whereas a maximum value of $\overline{C}_{pe}$ = 0.158 was found at the arch (a2) (i.e., at x/d = 0.02 and y/*l* = 0.19) in the model with gable end walls.

(v) For θ = 0º, the values of $\widetilde{C}_{pe}$ on the entire exterior surface of the roof of the model with gable end walls are high when compared to model with no gable end walls.

(vi) For θ = 330º, 315 and 300º, an increasing trend was observed in the variation of $\widetilde{C}_{pe}$ from x/d = 0.02 to 0.98 for both conditions, whereas for θ = 270º decreasing trend was observed for the entire roof.

6. COMPARISON OF MEASURED 'C_{pe}' WITH LITERATURE VALUES

Comparison of C_{pe} for wind directions (i) parallel and (ii) perpendicular to the axis of the roof, which are given in national/international codal provisions/published data with the values obtained from the present wind tunnel model study are not straightforward, because they depend upon: (a) curvature of the roof and its surface roughness; (b) dimension (f, d, h and *l*) of the structure; (c) angle of wind incidence; (d) area over which the pressure coefficients are averaged, (e) reference height at which the velocity have to be considered to compute pressure coefficients and (f) flow characteristics (turbulence of the incident flow, wind profile). For example, with regard to reference height (h_{ref}), it is being considered as eaves height or average height of the roof or crown of the roof.

Nevertheless, comparison on $\overline{C}_{pe}$ between the present wind tunnel model (f/d = 0.245, h/d=0.021 and *l*/d = 1.01) study with gable end walls and the corresponding values recommended in various national/international codes at the specified regions is made for flow direction (i) parallel and (ii) perpendicular to the ridge and discussed in the following sections.

(a) For wind direction parallel to the axis of the roof:

- The IS: 875 (Part 3)-1987 [1] code specifies the value of C_{pe} is equal to −0.7 for the full width of the roof over a length of *l*/2 from the gable ends and −0.5 for the remaining portion.
- The AS/NZS: 1170.2: 2002 [2] specifies values of $C_{p,e}$ = −0.9, −0.4 upto a horizontal distance of 1h from windward edge and values of $C_{p,e}$ = −0.2, 0.2 at a

horizontal distance greater than 3h (h = average height of the roof) from the windward edge, for h/d ≤ 0.5.

- The ASCE/SEI 7-05 [3] specifies values of C_p = −0.9, −0.18 upto a horizontal distance of 1h from windward edge, gradually reduces to values of C_p = −0.3, −0.18 at a horizontal distance greater than 2h (h = average height of the roof) from the windward edge, for h/d ≤ 0.5.
- The AIJ Recommendations [4] gives C_{pe} values based on regions viz. 'R_a' (i.e., at a horizontal distance of 0.5*l* from windward edge), 'R_b' (i.e., next 1*l* distance from 0.5l) and 'R_c' (i.e., remaining portion of the roof in the longitudinal direction), where *l* = smaller of 4H and B; H = reference height (i.e., average roof height) and B = building width. For the ratios of present study, the corresponding values of C_{pe} for the regions of R_a, R_b and R_c are found to be −1.126, −0.619 and -0.4, respectively.
- The User's Guide NBC 1995 [5] and International Standard [7] specifies a value of C_p = −0.8 at windward edge, gradually reduces to a value of C_p = −0.1 at leeward edge, for h/d = 0.08.
- The Cook's designer's guide [6] recommends a value of C_{pe} = -0.15 for both the edges and −0.733 at the ridge portion, which are applicable to 1/10th length at the windward region along the longitudinal direction. For other regions beyond 1/10th length, value of C_{pe} is ranging from −0.704 to ±0.2.
- From the present wind tunnel model study, it is observed that the entire exterior surface of the roof is subjected to suction, a value of $\overline{C}_{pe}$ = −1.221 at the windward arch (a1) and gradually becomes lower value of $\overline{C}_{pe}$ = −0.24, at the leeward arch (a8), and this distribution/trend (not magnitude) is being found in [1, 3, 4, 5 and 7].

(b) For wind direction perpendicular to the axis of the roof:

According to various national/international codes of practice, for model with f/d = 0.245, h/d = 0.021 (roof on elevated structure) and *l*/d = 1.01, the values of C_{pe} are given in Table 1 and the values of C_{pe} for h/d = 0 (roof springing from ground level) are also given in Table 1. In order to avoid the ambiguity of the results, the values given in the Table 1 as "present study" are corresponds to values obtained from the center arch (a4) of the roof of the present wind tunnel model. From Table 1 the following observations were made:

(i) The pressure coefficients obtained from present study and AIJ recommendations [4] indicate a negative value at windward region of the roof.

(ii) The pressure coefficient distribution trends obtained from present study for the regions of centre half and leeward quarter has been similar to various national/international codes of practice, but varying in magnitudes.

(iii) The value of C_{pe} at the leeward quarter from various codes reasonably compare with the measured value.

(iv) The pressure coefficient distribution trend given in NBC [5] and ISO 4354 [7] has

been similar to present study, except the last l/6th span at the leeward region.

Table 1: Comparison between C_{pe} values for curved roofs

Regions →	**Windward quarter**		**Centre half**	**Leeward quarter**	**Remarks**
Codes ↓	**Roof springing from G. L.**	**Roof on elevated structure**			
IS [1]	$0.345^{\#}$	$-0.520^{\#}$	$-0.945^{\#}$	−0.400	$^{\#}$ *g*(f/d)
AS/NZS [2]	$0.094^{@}$ or 0.0		$-0.668^{@}$ or 0.0	$-0.346^{@}$ or 0.0	$^{@}$ *g*(h_{ave}/f)
ASCE [3]	0.343^{*}	0.068^{*}, -0.630^{*}	-0.945^{*}	−0.500	* *g*(f/d)
AIJ [4]		$-0.239^{\%}$	$-1.130^{\%}$	$-0.500^{\%}$	$^{\%}$ *g*(f/d; h/d)
CHINA [8]	$0.260^{\$}$	$0.090^{\$}$	−0.800	−0.500	$^{\$}$ *g*(f/d)
EN [9]	$0.385^{\&}$	$-0.100^{\&}$ / $-0.830^{\&}$ (h/d ≥ 0.5)	$-0.950^{\&}$	$-0.400^{\&}$	$^{\&}$ *g*(f/d, h/d)
Present study		-0.250^{+}	-0.740^{+}	-0.52^{+}	$^{+}$ *g*(f/d, h/d & l/d)

Note: h_{ave} = average roof height; **g*(f/d) = Value of C_{pe} is a *function* of rise to span ratio (typical)

Regions → **Codes ↓**	E	F	G	H	J	K
NBC [5] & ISO 4354 [7]	−0.1	−0.5	−0.8	−0.8	−0.4	−0.1
Present study	−0.16	−0.70	−0.76	−0.74	−0.58	−0.57

7. SUMMARY AND CONCLUSIONS

Based on wind tunnel experiments conducted on a scaled (1:200) model of an industrial structure with multi-segmental curved roof, this paper presents results on measured mean and standard deviation of internal and external pressure coefficients on the entire roof of the model with and without gable end walls for angles of wind incidence from θ = 0º to 270º (i.e., flow direction from parallel to perpendicular to the ridge). Comparison on values of C_{pe} obtained from the present study and the values given in national/international codes of practice were made. Further, the effect of gable end walls on $\overline{C}_{pe}$ and $\widetilde{C}_{pe}$ of the roof surface was also studied and presented in this paper. The results of the experimental study leads to the following conclusions:

(i) For wind direction parallel (θ = 0º) to the axis of the roof, the entire roof of the model is subjected to suction and high at the windward arch (a1) and gradually becomes low at the leeward arch (a8), especially for model with gable end walls and this trend is being observed in the codal recommendations of [1, 3, 4, 5 and 7].

(ii) In the variation of $\overline{C}_{pe}$, for wind direction perpendicular (θ = 270º) to the axis of the roof, it is observed that a small portion in the windward region is subjected to suction as predicted by AIJ recommendations [4], high suction at the centre region and relatively low suction at the leeward region, which is also observed in many of the codal recommendations.

(iii) The value of C_{pe} at the leeward quarter from various codes reasonably compare with the measured value.

(iv) The pressure coefficient distribution trend given in NBC [5] and International Standard [7] has been similar to present study, except the last $l/6^{th}$ span at the leeward region.

(v) It is observed from the measurement that high suction on the roof was occurred for a skewed wind incidence (θ = 300º) with a value of $\overline{C}_{pe}$ = -1.433, which is well above those that are realised with wind blowing parallel ($\overline{C}_{pe}$ = −1.221) or perpendicular ($\overline{C}_{pe}$ = −1.118) to the axis of the roof.

(vi) For θ = 300º, a maximum value of $\overline{C}_{pe}$ = −1.09 at the downstream of apex of the centre arch (a4) was observed in the model with no gable end walls whereas a maximum value of $\overline{C}_{pe}$ = −1.433 was found at the downstream of apex of the arch (a1) in the model with gable end walls, at the same location (i.e., at x/d = 0.75 and y/*l* = 0.56).

(vii) For skewed angle of wind incidence (θ = 300º), a maximum value of $\widetilde{C}_{pe}$ = 0.282 is observed at x/d = 0.68 and value of $\widetilde{C}_{pi}$ (or $\widetilde{C}_{pe}$) are relatively higher at arch (a1) when compared to other arches for both cases i.e., with and without gable end walls.

Acknowledgements: This paper is published with the kind permission of the Director, CSIR-SERC, Chennai. The support rendered by the staff of Wind Engineering Laboratory towards conducting the wind tunnel experiment including fabrication of the model is sincerely acknowledged.

REFERENCES

1. IS: 875 (Part 3)-1987. Indian Standard Code of Practice for Design Loads (Other than Earthquake) for Buildings and Structures, Part 3, Wind Loads, Bureau of Indian Standards, New Delhi, 1989.
2. AS/NZS: 1170.2: 2002. Australian/New Zealand Standard, Structural design actions, Part 2: Wind actions, Standards Australia & Standards New Zealand, 2005.
3. ASCE/SEI 7-05. Minimum design loads for buildings and other structures, American Society of Civil Engineers Standard, 2006.
4. AIJ recommendations for loads on buildings, Architectural Institute of Japan, Japan, 2004.
5. User's Guide-NBC: 1995. Structural commentaries (Part 4), NRC-CNRC, Canadian Commission on Building and Fire Codes, National Research Council of Canada, 2002.
6. Cook NJ. The designer's guide to wind loading of building structures, Part 2 Static structures, Butterworths, London, 1990.
7. ISO 4354. Wind actions on structures, International Organization for Standardization, 1997.
8. GBJ 9-87. National standard of the people's republic of China, Load code for the design of building structures, New World Press, Beijing, 1994.
9. EN1991-1-4. Eurocode 1: Actions on Structures-Part 1-4: General actions-Wind actions, 2004.
10. Krishna P. Wind loads on curved roofs, Proceedings of the Second Asia Pacific Conference on Wind Engineering (APCWE-II), Beijing, China, 1989, pp. 39-53.
11. Kasperski M. Design wind loads for arched roofs, *Proceedings of the Fourth National Conference on Wind Engineering*, Structural Engineering Research Centre, Chennai, India, 2007, pp. 57-74.
12. Blackmore PA, Tsokri E. Wind loads on curved roofs, *Journal of Wind Engineering and Industrial Aerodynamics,* No. 11, **94**(2006) 833-44.
13. Franchini S, Pindado S, Meseguer J, Sanz-Andres A. A parametric, experimental analysis of conical vortices on curved roofs of low-rise buildings, *Journal of Wind Engineering and Industrial Aerodynamics,* No. 8, **93**(2005) 639-50.
14. Holmes JD. Determination of wind loads for an arch roof, *The Civil Engineering Transactions*, The Institution of Civil Engineers, Australia, 1984.
15. Paluch MJ, Loredo-souza AM, Blessmann J. Wind loads on attached canopies and their effects on the pressure distribution over arch roof industrial building, *Journal of Wind Engineering and Industrial Aerodynamics,* No. 8, **91**(2003) 975-94.
16. Ginger JD. Fluctuating wind loads across gable-end buildings with planar and curved

roofs, *Wind and Structures,* No. 6, **7**(2004) 359-72.
17. Blessmann J. Wind loads on isolated and adjacent industrial curved roofs, *Proceedings of the Jubileum Conference on Wind Effects on Buildings and Structures*, Porto Alegre, Brazil, 1998, pp. 137-171.
18. Biagini P, Borri C, Facchini L. Wind response of large roofs of stadions and arena, *Journal of Wind Engineering and Industrial Aerodynamics,* Nos. 9-11, **95**(2007) 871-87.
19. Del Coz Díaz JJ, García Nieto PJ, Suárez Domínguez FJ. Numerical analysis of pressure field on curved self-weighted metallic roofs due to the wind effect by the finite element method, *Journal of Computational and Applied Mathematics*, No. 1, **192**(2006) 40-50.
20. Gupta VK, Amareshwar K. Wind pressure distribution on buildings with circular roofs, *Proceedings of the Third National Conference on Wind Engineering*, Jadavpur University, Kolkata, India, 2006, pp. 375-379.
21. Robertson AP, Rouxb Ph, Gratraudb J, Scarasciac G, Castellanoc S, Dufresne de Vireld M, Palierd P. Wind pressures on permeably and impermeably-clad structures, *Journal of Wind Engineering and Industrial Aerodynamics,* Nos. 4-5, **90**(2002) 461-74.
22. Lakshmanan N, Arunachalam S, Selvi Rajan S, Abraham A, Ramesh Babu G. Wind pressure distribution on curved roof of an industrial shed with open end walls, *Proceedings of the Sixth Structural Engineering Convention,* Structural Engineering Research Centre, Chennai, India, 2008, pp. 1433-1442.
23. Abraham A, Arunachalam S, Selvi Rajan S, Ramesh Babu G, Lakshmanan N. Wind tunnel study on an industrial structure with curved roof, *Proceedings of the Seventh Asia-Pacific Conference on Wind Engineering*, Taipei, Taiwan, 2009, pp. 749-752.